Rayleigh-Benard Convection and Thermal Bifurcation in a Fluid Layer Subject to a Long Wavelength Heating

A. Asgarian[1], M. Z. Hossain[1], and J. M. Floryan[1]

[1]*Department of Mechanical and Materials Engineering, The University Of Western Ontario, London, ON, Canada N6A 5B9*

Email: *aasgaria@uwo.ca*

Abstract

The present work deals with the natural convection in a horizontal slot whose bottom is subject to a spatially periodic heating and the upper wall is kept isothermal. This type of heating results in the appearance of hot and cold zones along the slot length, and initiates primary convection regardless of the magnitude of the heating. It has been shown that the primary convection has a simple topology consisting of one pair of counter-rotating rolls per heating period when the heating intensity does not exceed the critical value of Ra_{cr} = 427. An explicit solution describing such flow structures has been developed

The main analysis is focused on the heating with the wavelength that is large when compared with the slot opening (small wave number limit). In this case, secondary motions in the form of rolls aligned in the direction of primary rolls and concentrated around the hot spots emerge for more intense heating ($Ra > Ra_{cr}$). This results in bifurcation of new solutions corresponding to secondary convection with different topologies. When $427 < Ra < \sim 470$ the secondary motions form the "supercritical pitchfork bifurcations" and can occur only if the heating wave number α is reduced below ~0.14. Increase of heating intensity to $Ra > \sim 470$ results in secondary motions occurring at larger values of α, i.e. $\alpha > \sim 0.14$, and bifurcations change character into "bifurcations from infinity". The bifurcation processes are insensitive to variation of the Prandtl number for $Pr \approx 0(1)$.

1. Introduction

Natural convection in layer of fluid has received considerable attention as it is the most common fluid flow in universe [1] and has several applications such as industrial appliances (compact heat exchangers), electronic component cooling, crystallization processes, chemical vapour deposition, weather prediction (atmospheric motions and clouds), motion of oceans, dynamics of the interiors of planets and stars (granulation of the sun), evolution of galaxies, etc. Over more than a century, numerous investigations have been done on the subject of classical problem of the Rayleigh-Benard convection (RBC) and various convective patterns have been observed by researchers [2]. In fact, RBC problem is known as a typical example of gradual transition from laminar to turbulent regime which can occur through several (known and unknown) routes and successive bifurcations.

Since in reality boundary imperfection either in terms of geometry or in terms of distribution of temperature is inevitable, recent efforts have been directed toward analysis of the effects of imperfections in boundary conditions and the resulting modulation of the RBC problem. In addition, the external modulation can be viewed as an effective tool to control the convection scenarios and pattern formation.

The analytical studies of modulated RBC problem have been done by Kelly and Pal [3,4] who considered both types of modulation, i.e. (i) spatially modulated temperature and (ii) spatially periodic geometry. Their analytical argument suggests that these two cases can be satisfactorily mapped to each other provided that amplitude of modulation is small and Ra is close to Ra_{cr}. Riahi [5] studied the problem of weakly nonlinear thermal convection while “two-dimensional” modulated temperature was prescribed at both boundaries with different fixed mean temperatures. His study has an important message: pattern formation for modulation on both boundaries can be quite distinct from modulation on one boundary; this is due to linear combination of the modulation modes on different boundaries. Hossain and Floryan [6], also explored the occurrence of convection due to spatial distribution of heating with fairly small, moderate, and large wave number of heating on the fluids with a wide range of Prandtl number (10^{-2} <Pr <10^3). A valuable insight into the RBC problem subject to modulated thermal boundary condition on the "lower" plane has been given by Freund et. all [7]; the governing Oberbeck-Boussinesq equations were solved via direct numerical solution. They have presented the stability diagram (for certain range of *Ra*, wave number α, and for small amplitude of modulation) in the plane of *α* - *Ra*.

In this work, we aim to complete the previous investigations on this subject ([3-7]) by extending analysis toward small and very small heating wave numbers (0.01< *α* <0.5). Results are presented for two values of the Prandtl numbers: Pr=0.71 (air) and 7 (water).

2. PROBLEM FORMULATION

Consider a layer of fluid confined between two infinite parallel plates placed apart each other at distance 2d as shown in Fig.1a. The upper wall is kept at a constant temperature while the lower wall is subjected to a spatially distributed heating. Note that the heating pattern is such that both walls have the same mean temperature. Fig.1b shows the temperature distribution on the lower wall presented in terms of θ, where $\theta = T - T_U$, and T_U is the upper wall temperature.

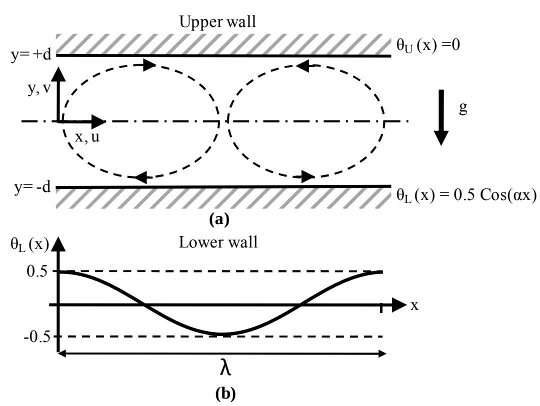

Fig.1 Parallel plates subject to a periodic heating imposed at the lower wall.

The flow is assumed to be steady and the working fluid satisfies the Boussinesq approximation. The spatial pattern of heating is well parameterized by the heating wave number (α), the amplitude of the heating is specified in terms of a suitably defined Rayleigh number ($Ra = g\beta T_d d^3 / \nu\kappa$), and fluid properties are described in terms of the Prandtl number ($\Pr = \nu / \kappa$). In the above, g is the gravitational acceleration, β is the thermal expansion coefficient, T_d is the peak-to-peak amplitude of temperature variations prescribed along the lower plate, d is the half of channel opening, ν is the kinematic viscosity, and κ is the thermal diffusivity.

The governing equations are the continuity, the stream function form of Navier-Stokes, and the energy equations (for more details see [6]).

3. METHODS OF SOLUTION

Since in numerical simulation there is some uncertainty about the accuracy of results, we have carried out solution using different methods in order to ascertain the validity of the results. Three numerical techniques including Spectral Chebyshev-Collocation, Variable-Step-Size Finite-Difference, and Finite-Volume Methods have been used to solve the governing equations. Results produced by all these three solvers identify the same characteristics of convection in the zone where multiplicity of solutions exists. Besides, an asymptotic solution has been developed for the limit $\alpha \rightarrow 0$; its testing demonstrated good consistency with the numerical results. For the sake of continuity and more emphasis on physical aspects, the final asymptotic solution of field quantities is given in Appendix A.

4. DISCUSSION OF RESULTS

4.1 Primary Convection

The primary response of the system appears in the form of two counter rotating rolls for each wavelength of the heating. This convective scenario can be obtained by asymptotic approach for the limit of α→0.

The conductive temperature field generates a buoyancy force acting upwards at x=0 and downwards at $x = \lambda/2$; this force is responsible for driving the fluid upwards at x = 0 and downwards at $x = \lambda/2$ and leads to the formation of the rolls displayed in Fig.2.

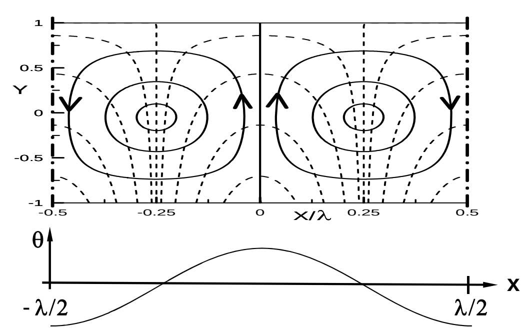

Fig.2 Typical topology of stream-lines (solid lines) and isotherms (dash lines) for primary convection.

The reader should note that convection creates temperature modifications ($\hat{\theta}$) that consist of a non-periodic term that is responsible for the generation of a net heat flow between the plates and a second harmonic of the imposed heating; there is no component with the same periodicity as the imposed heating.

Figures 3a-b illustrate variations of the relative error of the asymptotic solution as a function of α and Ra, respectively. This provides a quantitative measure of the range of validity of the asymptotic solution.

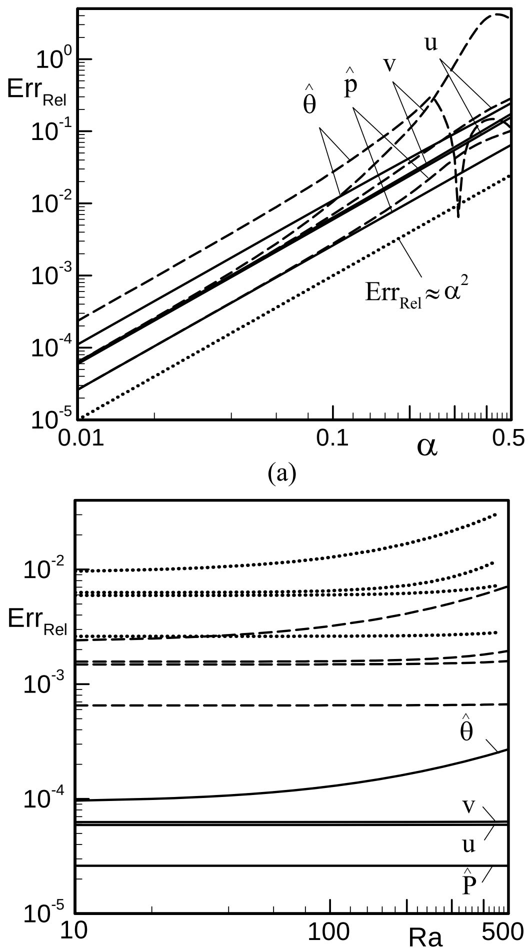

(a)

(b)

Fig.3 Variations of the relative error of the asymptotic solution for a fluid with Pr=0.71 as a (a) function of the heating wave number α for selected values of the Rayleigh number Ra (Ra= 50 - solid lines, Ra = 400 - dash lines) and (b) as a function of the Rayleigh number Ra for selected values of the heating wave number α (α = 0.01 - solid lines, α = 0.05 - dash lines; α = 0.1 - dotted lines). The dotted line with slope ~α2 is shown for reference purposes.

The error is defined as

$$\mathrm{Err_{rel}} = \underbrace{\max}_{-1<y<1}\left|\frac{|q_{num}|-|q_{asym}|}{|q_{num}|}\right|, \tag{4.1}$$

where q stands either for u evaluated at $x = \lambda/4$ or for any of the remaining quantities evaluated at $x = \lambda/8$ (λ=2π/α is wavelength of heating), and subscripts "num" and "asym" denote quantities computed on the basis of the complete and asymptotic equations, respectively. It can be seen that the relative error is less than 0.1 for $\alpha \approx 0.2$ even when $Ra = 400$.

4.2 Secondary Convection

The primary quantity of interest in the analysis of convection is the net heat transfer across the slot which can be expressed in terms of the global (mean) Nusselt number based on the conductive temperature scale (T_d)

$$\overline{\mathrm{Nu}} = \frac{\mathrm{Pr}}{\lambda}\int_0^{\lambda}\left(-\left.\frac{d\theta}{dy}\right|_{y=-1}\right)dx, \tag{4.2}$$

which takes the following form for asymptotic case:

$$\overline{\mathrm{Nu}}_{asym} \to \alpha^2\mathrm{Ra}/1400 \quad \text{when} \quad \alpha \to 0. \tag{4.3}$$

Figure 4 illustrates variations of $\overline{\mathrm{Nu}}/Ra$ as a function of α for selected values of Ra. It can be seen that variations of $\overline{\mathrm{Nu}}$ can be predicted using asymptotic theory as long as Ra < 427 (lines of these cases are overlapped with asymptotic line in Fig.4). When Ra > 427, $\overline{\mathrm{Nu}}$ branches off and approaches other asymptotic, Ra-dependent limits as $\alpha \to 0$.

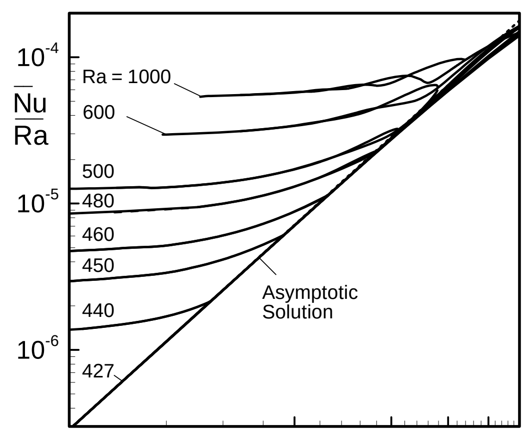

Fig.4 Variations of the mean Nusselt number as a function of the heating wave number α for selected values of the Rayleigh number.

For the case of small heating wave number α, i.e. long wavelength of heating, small zones on both sides of hot spots are subject to an almost uniform heating. Therefore, if the magnitude of the heating is sufficiently large ($Ra > Ra_{cr}$), the zones around the hot spots may experience the Rayleigh-Benard-type instability. The classical critical Rayleigh number expressed in terms of thickness of the slot for a uniformly heated wall is $Ra_{cr\text{-}classical} = 1708$ (see [2]). This number expressed using the present scaling takes the value $Ra_{cr} = 427$. The numerical results suggest that the thermal instability does take place provided that both α is sufficiently small and Ra exceeds the Ra_{cr} at the same time. In this case, secondary rolls emerge 'only' locally around the hot spots and results in bifurcation in the solution. Two types of secondary convective pattern have been determined: (1) the one with the first roll, the roll closest to the hot spot, rotating counter-clockwise (in the opposite direction of the primary roll) as shown in Fig.5c, and (2) the one with the first roll rotating clockwise (Fig.5d). The reader may note that we have focused our attention on the half of the wavelength on the right side of x=0 (the region marked in Fig.5b by box) and all nomenclature and roll counting refer to this region.

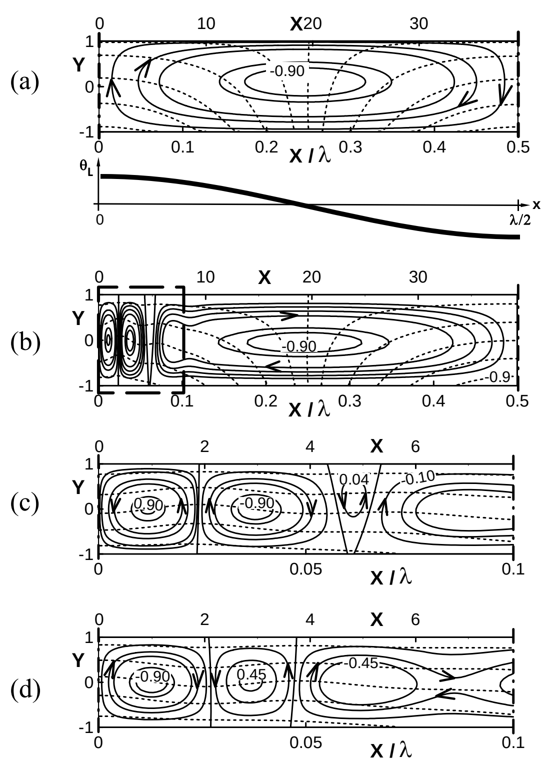

Fig.5 Flow structures for heating with *Ra*=450 and *α* = 0.08. Fig.5a depicts the primary convective pattern and the temperature distribution on the lower wall. The remaining figures correspond to the existence of secondary convective rolls (Fig.5b - odd number of rolls, Fig.5c - enlargement of the box in Fig.5b, and Fig.5d - even number of rolls). Solid and dash lines correspond to streamlines and isotherms, respectively.

The other characteristic which makes two types of flow structure completely different is the number of rolls. The one shown in the Fig.5c always has an odd number of rolls while the other one (Fig.5d) always comprises of an even number of rolls. Decrease in the heating wave number leads to nucleation of new rolls, however, both types of structures maintain their characteristics as the new rolls always emerge in pairs.

4.3 Pitchfork Bifurcation

The fact that there may be more than one solution for the same problem with exactly the same boundary conditions arises from the nonlinearity of field equations. The appearance of multiple solutions is referred to as bifurcation and is associated with a change in the qualitative character of the system (e.g. flow structure) and quantitative measure (e.g. Nusselt number). At this instant, we switch to the local Nusselt number at the hot spot as a quantity which well measures the properties of the flow system for the analysis of the branching process. This number is defined as

$$Nu_L = -Pr\left.\frac{d\theta}{dy}\right|_{x=0,\ y=-1}.$$

Variation of Nu_L for "supercritical" value of *Ra*=450 is illustrated in Fig.6.

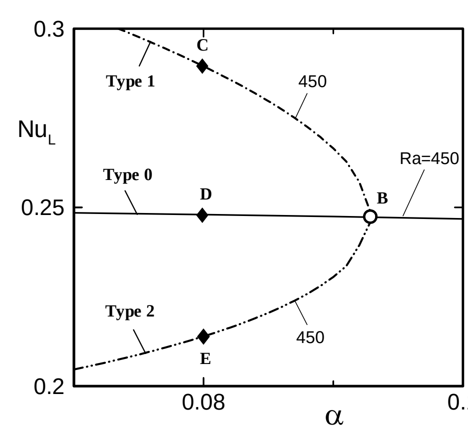

Fig.6 Variations of Nu_L as a function of the heating wave number α for fluid with Pr=0.71 subject to heating corresponding to the Ra=450. Points C, D, and E correspond to the same wave number α=0.08 but belong to branches of type 1, 0 and 2, and their corresponding flow structures displayed in Fig.3c, Fig.3a, and Fig.3d, respectively.

It can be seen that when α > 0.092 (point B), the solution is unique. But once the heating wave number decreases below the critical value of 0.092, a pitchfork bifurcation composed of three branches is found.

For convenience we shall call solutions corresponding to the middle, upper and lower branches as branches of type 0, 1, and 2, respectively. Branch of type 0 has a simple topology involving one large flow cell extending over half period of heating with the fluid moving upwards above the hot spot (Fig.5a). For branch of type 1, flow re-arrangement begins with the formation of a small separation bubble at the upper wall above the hot spot which grows (as α decreases) to form a secondary roll attached to the hot spot. The secondary roll rotates in the counterclockwise direction and thus brings colder fluid into contact with the lower wall resulting in an increase of Nu_L. Further decrease of α results in a sequential formation of additional pair of rolls; this lets the branch of type 1 to always have an odd number of rolls. The same process occurs along the branch of type 2 with one exception, i.e., when we cross the critical point, two secondary rolls (rather than just one) appear to be followed by formation of additional rolls always in pairs resulting in an even number of rolls.

4.4 Bifurcation from Infinity

We shall now switch our attention to higher values of *Ra*, i.e., *Ra* > ~470, where changes in the flow structures correspond to "bifurcations from infinity" as shown in Fig.7. For convenience we shall refer to solutions corresponding to the finite and infinite branches as branches of types 3 and 4, respectively.

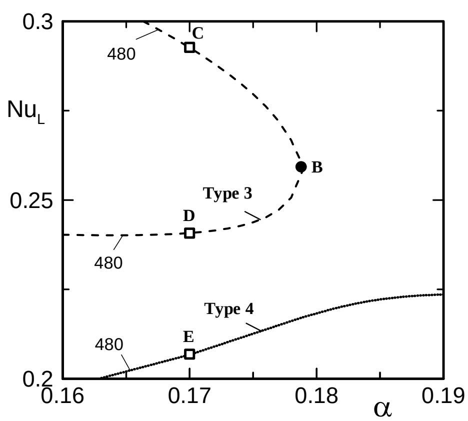

Fig.7 Variations of the local Nusselt number as a function of the heating wave number α for a fluid with the Prandtl number Pr=0.71 subject to heating corresponding to the *Ra*=450.

At the left limit of the lower part of branch of type 3, flow forms one roll as shown in Fig.8b. Increase of α (moving along the branch to the right toward critical point B with α = 0.178) results in initiation of the formation of a secondary roll rotating in the direction opposite to the direction of the primary roll. The process of formation of new rolls is similar to that observed in the case of branch of type 1 resulting in the creation of an odd number of rolls as shown in Fig.8a. At the right limit of branch of type 4, the motion consists of only primary convection. A decrease of α (moving to the left of α = 0.178) leads to formation of secondary rolls. Fig.8b gives a picture of in-flow stagnation phenomenon which is the starting point for the formation of two secondary rolls. Further decrease in α leads to the process very similar to that observed in the case of branch of type2 with even number of rolls.

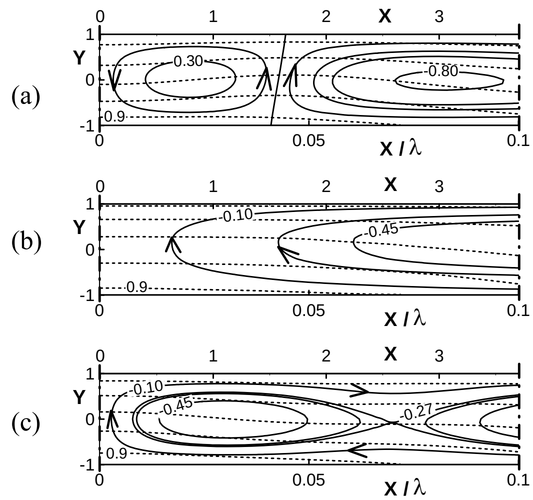

Fig.8 Flow structures for heating with *Ra*=480. and α = 0.17. Flow conditions in Fig.6a-c correspond to points C, D, and E in Fig.5, respectively. Solid and dash lines correspond to streamlines and isotherms, respectively.

4.5 Comprehensive Bifurcation Diagram

To have better perspective of the bifurcation process in the global parameter space, changes in the form of secondary motions have been traced by constructing two comprehensive bifurcations diagrams: (i) in the (α, Nu_L) plane for fixed values of *Ra* as shown in Fig.9 and (ii) in the (*Ra*, Nu_L) plane for fixed values of α as shown in Fig.10, and thus permit creation of a global diagram in the (α, *Ra*, Nu_L) space. In both figures, open circles identify critical conditions for pitchfork bifurcations and filled circles identify critical conditions for "bifurcations from infinity".

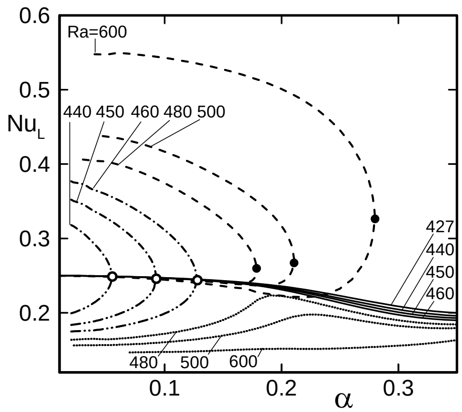

Fig.9 Variations of the local Nusselt number Nu_L at $x = 0$, $y = -1$ as a function of the heating wave number α for a fluid with the Prandtl number Pr=0.71 subject to heating corresponding to the supercritical values of the Rayleigh number ($Ra > 427$). Solid, dash-dot, dash-dot-dot, dash, and dot lines correspond to bifurcation branches of types 0, 1, 2, 3, and 4 respectively.

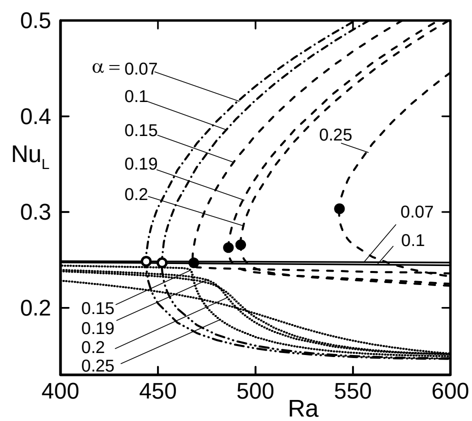

Fig.10 Variations of the local Nusselt number Nu_L at $x = 0$, $y = -1$ as a function of the Rayleigh number for selected values of the heating wave number α for a fluid with the Prandtl number Pr=0.71. Solid, dash-dot, dash-dot-dot, dash, and dot lines correspond to bifurcation branches of types 0, 1, 2, 3, and 4, respectively.

If one transfer all the critical points marked in Fig.9 and Fig.10 into the Ra-α diagram, the resulting plot shows variations of the critical Rayleigh number Ra_{cr} as a function of α (Fig.11). It can be seen that decrease of α results in Ra_{cr} approaching the limit of 427, which agrees with the critical conditions for the Rayleigh-Benard instability for a uniformly heated lower wall [2]. An increase of α leads to the primary convection with a strong spatial modulation and results in a rapid increase of Ra_{cr}. Other forms of instability may occur under such conditions but will require more intense heating, i.e. higher values of Ra.

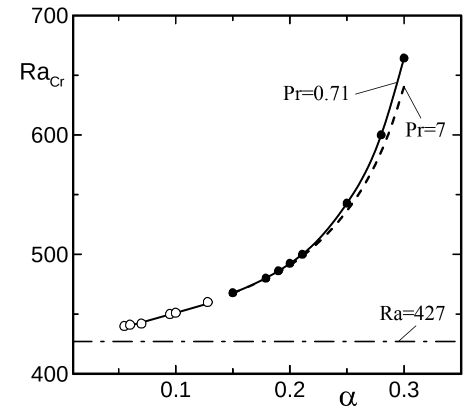

Fig.11. Variation of the critical Rayleigh number Ra_{cr} as a function of the heating wave number α for fluids with Pr=0.71 and Pr = 7. Open circles denote critical conditions for the pitchfork bifurcations and filled circles denote the critical points for the "bifurcations from infinity".

4.6 Effect of Prandtl Number

It is of interest to inquire how changes of the Prandtl number may affect the system response. For this reason the variation of Nu_L for wide range of α (which includes pitchfork bifurcation, bifurcation form infinity, and subcritical primary convection) is analyzed for values of Pr corresponding to air and water, i.e., Pr = 0.71 and Pr = 7. Comparison of results displayed in Fig. 12 demonstrates that bifurcation process is almost insensitive to variations of the Prandtl number for Pr = 0(1) as only small differences are observed between results for Pr = 0.7 and Pr = 7.

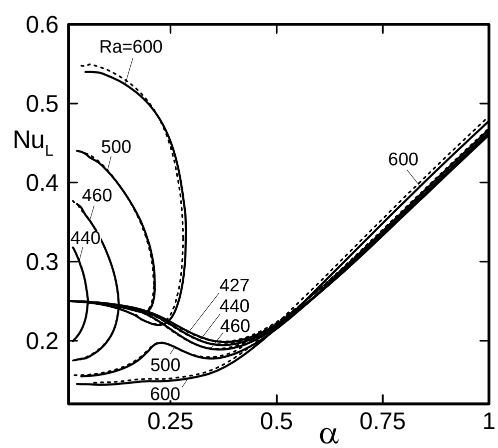

Fig. 12 Variations of the local Nusselt number Nu_L as a function of the heating wave number α for selected values of the Rayleigh number for fluids with the Prandtl numbers Pr = 0.71 (dash lines) and 7 (solid lines).

5. CONCLUSION

We have studied natural convection in an infinite horizontal slot subject to periodic heating with heating wavelength that is large when compared with the slot opening. It has been shown that convection has a simple topology consisting of one pair of counter-rotating rolls per heating period when the Rayleigh number *Ra* does not exceed the critical value of 427. When the heating intensity is larger than the critical value but not too large, i.e., 427 < *Ra* < ~470, the secondary motions correspond to supercritical pitchfork bifurcations and occur only if α is sufficiently small, i.e., $\alpha < \sim 0.14$. Increase of heating intensity to *Ra* > ~470 results in the secondary motions occurring at larger values of α, i.e. $\alpha > \sim 0.14$, and bifurcation changing character to "bifurcations from infinity".

The bifurcation processes are insensitive to variations of the Prandtl number for Pr = 0(1) as only small differences have been observed between results for Pr = 0.7 and Pr = 7. It has been shown that the observed phenomena are strictly associated with the small wave number limit of the external heating.

6. REFERENCES

[1] K.A. Emanue, "Atomospheric Convection", *Oxford Univ. Press, New York*, 1994

[2] P. G. Drazin, "Introduction to Hydrodynamic Stability", *Cambridge Univ. Press, New York*, 2002

[3] R. E. Kelly and D. Pal, "Thermal convection with spatially periodic boundary conditions: resonant wavelength excitation", *J. Fluid Mech.* 86, p433, 1978

[4] D. Pal and R. E. Kelly, "Thermal convection with spatially periodic nonuniform heating: nonresonant wavelength excitation", *Proc. 6th Int. Heat Transfer Conf., Toronto*, p235, 1978

[5] D. N. Riahi, "Finite amplitude thermal convection with spatially modulated boundary temperatures", *Proc. R. Soc. Lond*. A 449, 459 1995

[6] M. Z. Hossain and J. M. Floryan, "Roll Instability of a Stationary Fluid Exposed to Spatially Distributed Thermal Forcing", *18th annual Conf. of CFDSC, London*, 2010

[7] G. Freund, W. Pesch, and W. Zimmermann, "Rayleigh-Benard convection in the presence of spatial temperature modulations", *J. Fluid Mech.* Published online 24 Feb 2011

APPENDIX A

For the limit α→0, the asymptotic solutions for pressure field, u- and v-velocity, conductive temperature, and convective temperature take the following forms, respectively:

$$\hat{P} = (\frac{Ra}{\Pr})(\frac{1}{4})\cos(\alpha x)\left[-\frac{1}{2}y^2 + y + \frac{1}{10}\right] + 0(\alpha^2), \qquad (A.1)$$

$$u = -\alpha(\frac{Ra}{\Pr})(\frac{1}{4})\sin(\alpha x) \left[-\frac{1}{24}y^4 + \frac{1}{6}y^3 + \frac{1}{20}y^2 - \frac{1}{6}y - \frac{1}{120}\right] + 0(\alpha^3), \qquad (A.2)$$

$$v = \alpha^2(\frac{Ra}{\Pr})(\frac{1}{4})\cos(\alpha x) \left[-\frac{1}{120}y^5 + \frac{1}{24}y^4 + \frac{1}{60}y^3 - \frac{1}{12}y^2 - \frac{1}{120}y + \frac{1}{24}\right] + 0(\alpha^4), \qquad (A.3)$$

$$\bar{\theta} = \frac{1}{4}(1-y)\cos(\alpha x) + 0(\alpha^2), \qquad (A.4)$$

$$\hat{\theta} = a^2(\frac{Ra}{32\Pr})\left\{\left[\frac{1}{840}y^7 - \frac{1}{120}y^6 + \frac{1}{200}y^5 + \frac{1}{40}y^4 - \frac{1}{40}y^3 - \frac{1}{40}y^2 + \frac{79}{4200}y + \frac{1}{120}\right] - \left[\frac{1}{1260}y^7 - \frac{1}{180}y^6 + \frac{1}{150}y^5 + \frac{1}{90}y^4 - \frac{1}{36}y^3 + \frac{1}{60}y^2 + \frac{32}{1575}y - \frac{1}{45}\right]\cos(2\alpha x)\right\} + 0(\alpha^4), \qquad (A.5)$$

where the total temperature includes both conductive and convective fields as follows

$$\theta = \frac{1}{\Pr}\bar{\theta} + \hat{\theta}. \qquad (A.6)$$

For more details on the non-dimensionalization method and derivation of governing equations refer to [6].